C.P. No. 205
(13,878)

A.R.C. Technical Report

C.P. No. 205
(13,878)

A.R.C. Technical Report

MINISTRY OF SUPPLY

AERONAUTICAL RESEARCH COUNCIL

CURRENT PAPERS

Full Scale Measurements of Impact Loads on a Large Flying Boat

(Sunderland Mk.5)

Part II - Results for Impacts on Main Step

By

J. A. Hamilton

LONDON HER MAJESTY'S STATIONERY OFFICE

1955

FIVE SHILLINGS NET

C.P. No. 205

Report No. F/Res/220

February 1951

MARINE AIRCRAFT EXPERIMENTAL ESTABLISHMENT, R.A.F., FELIXSTOWE

Full Scale Measurements of Impact Loads on a Large Flying Boat (Sunderland Mk.5)

Part II - Results for Impacts on Main Step

by

J. A. HAMILTON

S U M M A R Y

Full scale measurements of landing impact forces and pressures have been made on the hull of a Sunderland Mk.5 flying boat (weight 50,000 lb) in order to provide basic information on the agreement between experiment and the latest available impact theories. The experiments were arranged to give impact conditions as near as possible to those assumed in theory.

The results revealed a marked discrepancy between the form of the total impact-time curve predicted by theory, and that measured on the aircraft. In particular, the measurement of time to reach maximum impact force was about twice that indicated by theory. The magnitudes of the theoretical and measured maximum impact forces were in reasonable agreement. This discrepancy may be attributable to the neglect of after-body influences in the theoretical analyses.

Measurement of the intensity of maximum hydrodynamic pressures on the planing bottom confirmed that pressure and velocity component normal to the keel may be related by an expression of the form

$$p_{max} = \frac{1}{2} \frac{\rho V_n^2}{K} \left[\left(\frac{\pi}{2} \cot \theta_L \right)^2 + 1 \right]$$

where

θ_L = the local deadrise angle in degrees

ρ = the density of water in slugs per cubic foot

V_n = the velocity at the time and position at which p_{max} is measured (f.p.s.).

The experimental value for K is 132 when p_{max} is given in p.s.i.

The distribution of pressure from the keel to the maximum pressure

/point .....

CONTENTS

/List of Appendices .....

LIST OF ILLUSTRATIONS

/Comparison .....

LIST OF SYMBOLS

K	Constant in Wagner's maximum pressure formula $p_{max} = \frac{1}{2}\rho \frac{V_n^2}{K} \left[\left(\frac{\pi}{2} \cot \theta_L\right)^2 + 1 \right]$
K_1	Associated mass factor
p	Hydrodynamic pressure p.s.i.
p_{max}	Maximum value of hydrodynamic pressure p.s.i.
W	Aircraft all up weight lb.
V_n	Velocity component normal to keel f.p.s.
V_T	Velocity component parallel to keel f.p.s.
$\frac{1}{y_o}$	$\frac{V_T \tan \tau}{V_{n_o}}$ (subscript o refers to conditions at initial impact)
η	$\frac{x}{c}$ where c is the wetted half beam and x the distance from the keel to the point at which pressure is being measured or deduced
θ	Deadrise of line joining keel to chine
θ_L	Local deadrise at any point on the hull planing bottom
τ	Incidence of keel to water surface

/Introduction .....

techniques and their accuracies and limitations, but merely as a summary sufficient to give coherence to the later discussion without necessitating reference to Part I of the report.

2.2.1. Total force measurement

The total impact force was measured by a number of variable inductance type accelerometers mounted at various positions along the wing span, Fig.2. In all, four accelerations were measured in each landing :-

(i) The acceleration at a point on the wing centre section (front spar, lower boom).

(ii) The acceleration at a point on the front spar, starboard wing, corresponding approximately to the nodal point of the fundamental wing vibration mode.

(iii) The acceleration at a point on the front spar, port wing, corresponding approximately to the nodal point of the fundamental wing vibration mode.

(iv) The resultant acceleration obtained from three accelerometers whose outputs were so combined as to eliminate the fundamental and first harmonic modes of wing vibration giving a final record of the hydrodynamic impact force modified by only higher modes of wing vibration (cf. Fig.2).

The necessity for this complication in measuring acceleration was indicated by the earlier structural tests[1] which showed that wing vibrations could modify severely the shape of the hydrodynamic impact acceleration-time curve. Acceleration measurement (i) gave merely the resultant hull acceleration including any wing vibration effects. Acceleration measurements (ii) and (iii) were intended to eliminate as simply as possible the wing fundamental mode and to indicate the effects of roll.

The principle behind accelercmeter measurement (iv) is fully described in Reference 1 where it was utilised to eliminate wing vibration modes from a centre section accelerometer record. For the present tests the scheme has been modified so that instead of obtaining the hydrodynamic impact acceleration-time curve from an analytical combination of three separate accelerometer records, the electrical outputs of the three accelerometers are combined in calculated proportions and the resultant output gives the required acceleration-time curve directly.

2.2.2. Planing bottom pressure measurements

Hydrodynamic pressure measurements were made on the forebody planing bottom by means of diaphragm type pressure pick-ups of the type used successfully for a similar purpose in the hull launching tank at M.A.E.E.[5,6] Briefly, the intensity of pressure at a point in the planing bottom is registered by the deflection of a thin, circular german silver diaphragm (1" diameter) fitted flush with the bottom skin. The diaphragm movement is transmitted mechanically to a small strain-gauged beam of beryllium-copper.

Twenty pick-ups were installed, all of them on the starboard side of the forebody (Fig.3).

/Each .....

3. Range of Tests and Piloting Technique

The primary objective of the tests was to obtain landing impacts which fulfilled as far as possible the conditions assumed in theoretical analyses. These are :-

(i) Zero normal (or vertical) acceleration prior to touchdown.

(ii) Zero drift velocity prior to touchdown.

(iii) Zero angle of roll during impact.

(iv) Zero angular velocity in pitch during impact.

(v) Main step only immersed.

The first of these conditions was usually satisfied by maintaining fixed elevator setting, power conditions and forward speed from a height of about 100 feet to the touchdown point. The second and third conditions apply to any good landing and were achieved by accurate handling of the aircraft in the approach. Unfortunately the pilot has little control over the fourth condition once the impact has started. Experience showed that with zero or slightly negative elevator angle an impact with zero pitching velocity was most likely to be achieved if the keel attitude at touchdown was in the region 2°-5°. Occasional pitching did occur even in this range however. The pilot can do little about condition (v) apart from ensuring that the main step touches first.

The requirements given to the pilot were, therefore :-

(i) Elevator fixed, engine power constant, forward velocity constant from 50-100 feet downwards.

(ii) Approach speed higher than usual in order to achieve a low attitude impact.

(iii) No check before touchdown.

No attempt was made to specify rate of descent because of the relative inaccuracy of the standard rate of descent meter. Landings were specified as heavier or lighter than the previous one. Most pilots did use the rate of descent meter as a guide during their approach. Frequently the aircraft bounced clear of the water after the first impact and pilots were encouraged to re-land straight ahead.

All the tests were made at one weight - 50,000 lb - and one centre of gravity position (3.0 feet forward of the main step point parallel to hull datum).

4. Weather Conditions

A calm sea was essential for this first investigation and fortunately during the 3 or 4 days occupied by the flight tests the wind strength averaged 3-4 knots with occasional gusts up to 8 knots. The sea surface was flat calm for the majority of landings, with a few made in 6" wavelets. Care was taken to allow ship washes to die away before landing.

5. Results

5.1. Total impact forces

The theoretical work of Reference 3 has been chosen as a suitable basis upon which to illustrate the variation of total hydrodynamic force

/with .....

The pressure distributions were less amenable to concise presentation than the maximum pressures. Two methods of obtaining experimental distributions have been employed. Figs. 10 and 12 show, plotted in non-dimensional form the transverse distributions obtained from pressures indicated simultaneously on several pressure pick-ups in rows A and B. The runs chosen for plotting are those for which reliable information is available from all the pressure pick-ups concerned.

Figs. 11 and 13 show transverse distributions obtained from the pressure time histories of one pick-up in each row by assuming that the pressure wave has a constant velocity past the pick-up for the time interval considered. The pick-ups plotted were chosen at random from all the results available. This second method was included because the first method, though more conventional and convenient, has the disadvantage that only three or four points on each distribution curve are known and slight calibration or response errors between individual pick-ups in the same row may cause scatter and thereby make the drawing of a fair curve through these isolated points difficult.

In all four figures, comparison is made with the theoretical distribution of Wagner's theory, given by the expression

$$p = \tfrac{1}{2}\rho V_n^2 \left[\frac{\pi \cot \Theta_L}{\sqrt{1-\eta^2}} - \frac{\eta^2}{1-\eta^2} \right]$$

where

$\eta = x/c$
c = wetted width
x = distance from keel

Owing to the difficulty of defining the wetted edge of the measured pressure wave, the maximum pressure position has been chosen as a common point for comparison of theoretical and experimental distribution. In Figs. 10 and 12 the distributions have been taken when the keel-maximum pressure distance was about 3 feet i.e. 0.6 beam. In Figs. 11 and 13 the peak pressure position has been made to coincide with the position of the pick-up being considered.

The pressure curves deduced by method one confirm the maximum pressure results in that the pressure magnitudes for row A lies slightly above the theoretical curve whereas those for row B lie on the theoretical curve or slightly below it. Figs. 11 and 13 give a more precise picture of the agreement between the shapes of distribution curve given by theory and experiment. There is good agreement in the region between keel and maximum pressure but the experimental curves show a slower build up from the wetted edge to maximum pressure.

5.3. Comparison with other theoretical and experimental investigations

5.3.1. Full scale experimental

A parallel series of full scale impact experiments was made by the N.A.C.A. on an amphibian having an all up weight of 20,000 lb and a main step deadrise of 20°.[7] The results from these tests were re-analysed on the basis of Reference 3 theory and they are presented in this form in Figs. 14 and 15.

The maximum impact accelerations follow the same trend as the British experimental-theoretical curve. Between values of $\frac{1}{y_o} = 0.6$ and $\frac{1}{y_o} = 0.8$ the experimental peak loads lie well above the theoretical curve, a fact which was noted in the original report and attributed to the effect of chine turndown in impacts where chine immersion occurred.

/The.....

Of these, the last may be immediately discounted since the curved portion is rarely immersed before the instant of maximum acceleration.

For all the computation of force parameters a mean deadrise of 26° was utilised although in practice the deadrise varies from 30° at the keel to 19° at the chine. To obtain some gauge of the effect of varying deadrise on the force-time curve, theoretical curves for typical impacts were calculated for a deadrise angle of 30° as well as 26°. These are compared with the experimental curves in Fig.7 and they confirm the small effect of deadrise variation between 26° and 30°.

In Reference 3 Crewe and Monaghan assume that the associated water mass for a wedge with a transverse step is proportional to the quantity

$$\frac{(\text{Area})^2}{\text{perimeter}}$$

and they further suggest that for a vee plan form their treatment should be used with the associated mass based on the appropriate value of

$$\frac{(\text{Area})^2}{\text{perimeter}}$$

This reasoning has been applied to several typical Sunderland impacts and the overall result is to bring about a decrease of 5% in the experimental values of B_o (non-dimensional time parameter) bringing the experimental points nearer the theoretical curve of Fig.6; and a similar increase in the experimental values of A_o bringing the experimental points further above the theoretical curve. (cf. Fig.5 and Appendix III).

6.1.2. Chine immersion

The presence of chine immersion appears to have no consistent effect on either maximum acceleration or time results (Figs. 5, 6 and 7). When it does occur, the chine immersion is small and takes place well after the theoretical time of maximum acceleration.

6.1.3. Hull and wing flexibility

For a complicated structure such as that of the Sunderland hull and wing, the effect of hull flexibility on the impact acceleration-time curve can only be computed by making preliminary estimates of various structural constants and then computing their effect by a laborious step by step method. Fortunately there are two items of experimental evidence which indicate that for these particular full scale impacts, hull and wing flexibility have little effect.

The first of these is illustrated in Fig.18 which compares the acceleration-time curves obtained from accelerometers at various points in the hull and wing for two typical impacts. These figures confirm that the wing vibrations were not sufficiently excited to produce appreciable differences up to the point of maximum acceleration.

The second piece of evidence is contained in Fig.14 of Reference 1 which shows that the effect of hull flexibility is negligible, certainly for the region near the main step.

6.1.4. Afterbody effects

The effect of the afterbody in modifying the simple impact theory has not received much notice in theoretical-experimental comparisons. It is significant, however, that the N.A.C.A. model tests which gave good agreement between theory and experiment in nearly every respect, were conducted on forebodies alone.

Two forms of afterbody interference are possible. In rear step first impacts, the afterbody absorbs some of the initial energy of impact and causes the hull to pitch forward onto the main step (Fig.8, Run 19).

/Landings .....

The difference between theory and experiment in the peak to wetted edge region may be attributed simply to differences in the physical conditions assumed by Wagner and those achieved in practice. The disagreement is of small significance in applying the results for purposes of structural design.

The exact shape of the measured wetted edge is interesting. Fig.19 shows that by the time the pressure wave reaches pick-up No. 18 of row A there is a region of low pressure before the rapid build-up towards the peak. This low pressure region will certainly invalidate any attempt to measure pressure areas and "splash up" values by means of water contact devices alone. Fig.20 illustrates the growth of such a low pressure area as the pressure wave proceeds towards the chine.

7. Design Implications

The detailed deduction of the design loads from basic theory is beyond the scope of this report and in any case the range of variables covered is too small to justify the general applicability of such deductions. However, the results do give rise to a few design problems which should be stated.

For the estimation of overall hydrodynamic impact loads, the theories of References 3 and 8 appear to give values which agree sufficiently closely with the measured results for the purpose of design. The discrepancy in times to maximum load is not serious per se, unless account has to be taken of the structural response to dynamic loads. However, it is disturbing in that it may imply a fundamental disagreement between theory and experiment, and the theoretical estimates should be used with some caution therefore, in applications where the conditions differ greatly from those of the present tests.

Unfortunately the time discrepancy affects the derivation of design frame and plating pressures to a much greater extent than it does the derivation of total impact load. For these, the theoretical formulae are given in terms of V_n, the local normal-to-keel velocity, and to be of design use some relationship must be found between ${}_oV_n$ - the initial normal to keel velocity, and V_n, or between ${}_oV_v$ and V_v since V_h is constant. Such a relationship may be obtained from the Reference 3 theory but this differs considerably from the experimental variations as the examples quoted in Fig.21 show.

The magnitude of the error in vertical velocity predicted for four typical landings is shown in Fig.22. Fig.23 shows that the corresponding errors in p and p_{max} may amount to 15-20% for values of V_v above $0.5V_{v_o}$.

The relationship between peak pressures - confined to a small planing bottom area - and design pressures over larger areas is examined in Appendix IV and a simple expression is there deduced for the relative magnitude of peak and mean distributed pressures. Fig.24 illustrates this with reference to a range of deadrise angles.

8. Conclusions

The form of impact force-time curve given by these full scale measurements differs from that indicated by current theories. In particular, the theoretical time to reach maximum impact force is almost half that given by measurement. The magnitudes of the theoretical and measured maximum impact forces are in good agreement. Some of these

/discrepancies ....

List of References

No.	Author(s)	Title, etc.
1	A. Burns A. J. Fairclough	Dynamic landing loads of flying boats. With special reference to measurements made on Sunderland TX. 293. R. & M. 2629. February, 1948.
2	J. A. Hamilton	A comparison between some full scale landing impact measurements and two impact theories. Report No. F/Res/211. A.R.C. 11,345. February, 1948.
3	P. R. Crewe R. J. Monaghan	Formulae for estimating the forces in seaplane water impacts without rotation or chine immersion. R. & M. 2804. January, 1949.
4	J. A. Hamilton	Note on a proposed programme for full-scale seaplane water impact tests. Report No. F/Res/212. A.R.C. 11,739. June, 1948.
5	J. W. McIvor	Full scale measurements of impact loads on a large flying boat. Part I - Description of apparatus and instrument installation. C.P. 182. March, 1950.
6	J. A. Hamilton J. W. McIvor	Measurements of impact pressures on the hull of a model seaplane. Report No. F/Res/215. A.R.C. 12,703. July, 1949.
7	Margaret F. Steiner	Comparison of overall impact loads obtained during seaplane landing tests with loads predicted by hydrodynamic theory. Report No. NACA/TN/1781. January, 1949.
8	Benjamin Milwitzsky	A generalised theoretical and experimental investigation of the motion and hydrodynamic loads experienced by Vee-bottom seaplanes during step landing impacts. Report No. NACA/TN/1516. February, 1948.
9	J. A. Hamilton	An investigation into the effect of after-body ventilation on the hydrodynamic characteristics of a small flying boat (Saro 37) with a 1:20 fairing over the main step. R. & M. 2714. November, 1947.
10	J. A. Hamilton	An interim report on the hydrodynamic performance of a large 4-engined flying boat (Sunderland Mk 5) with a 1:16.75 main step fairing. Report No. F/Res/214. A.R.C. 12,162. January,1949.
11	John D. Pierson	On the pressure distribution for a wedge penetrating a fluid surface. Stevens Institute of Technology Experimental Towing Tank Report No.336.

APPENDIX II

Wagner's Formulae for Distributed and Maximum Pressures on Hulls having Transverse Curvature

The general form of Wagner's formula for the distribution of hydrodynamic pressure across a hull is

$$p = \tfrac{1}{2}\rho V^2\left[\frac{2}{Q\sqrt{1-\eta^2}} - \frac{\eta^2}{1-\eta^2}\right] + \frac{dV}{dt}\cdot c\sqrt{1-\eta^2} \qquad (1)$$

For the landings under consideration in this report the expression $\frac{dV}{dt}\, c\sqrt{1-\eta^2}$ is small enough to be neglected without loss of accuracy.

From this modified equation may be deduced the Wagner expression for maximum pressure.

$$p_{max} = \tfrac{1}{2}\rho V^2\left[\frac{1}{Q^2} + 1\right] \qquad (2)$$

For a hull of constant deadrise

$$Q = \frac{2}{\pi}\tan\Theta$$

and expressions (1) and (2) become

$$p = \tfrac{1}{2}\rho V^2\left[\frac{\pi\cot\Theta}{\sqrt{1-\eta^2}} - \frac{\eta^2}{1-\eta^2}\right] \qquad (3)$$

$$p_{max} = \tfrac{1}{2}\rho V^2\left[\left(\frac{\pi}{2}\cot\Theta\right)^2 + 1\right] \qquad (4)$$

For simplicity in analysis expressions (3) and (4) have been applied to the Sunderland planing bottom and the effect of curvature has been allowed for by assuming that Θ is the value of the local deadrise at the point of the planing bottom being considered.

Let us examine the error involved in this assumption.

Wagner deduces [11] that for a hull of curved cross section

$$Q = \frac{2}{\pi}B_o + B_1 C + \frac{4}{\pi}B_2 C^2 \qquad (5)$$

where B_o, B_1, etc. are given by the equation for hull cross-section.

$$y = B_o x + B_1 x^2 + B_2 x^3 \qquad (6)$$

For the full scale tests it has been assumed that

$$Q \equiv Q_L = \frac{2}{\pi}\tan\Theta_L$$

where Θ_L is the local deadrise.

/From .....

APPENDIX III

Estimation of the Effect of a Vee-shaped Step on Total Impact Forces and Build-up Time

According to the theory of Reference 3 the non-dimensional impact load factor A_o is given by the expression

$$A_o = \frac{1}{K_1^{\frac{1}{3}}} \left(\frac{W}{\rho g}\right)^{\frac{1}{3}} \frac{dV_n}{dt} \Big/ V_{n_o}^{\ 2}$$

Of all factors on the right hand side $K_1^{\frac{1}{3}}$ is the only one directly affected by hull form and for fixed values of draft, attitude and deadrise

$$K_\alpha \frac{(\text{area})^2}{\text{perimeter}}$$

For a 24^o Vee plan shape, a mean deadrise of 26^o and a keel attitude of 5^o the ratio of K values is

$$\frac{K_1 \text{ vee}}{K_1 \text{ transverse}} = 0.86$$

i.e.

$$\left[\frac{K_1 \text{ vee}}{K_1 \text{ transverse}}\right]^{\frac{1}{3}} = 0.95$$

Hence the theoretical effect of a Vee-shape would be to increase the experimental values of Ao plotted in Fig.5 by approximately 5%.

Similarly, the non-dimensional time factor B_o is given by the expression

$$B_o = t_m \frac{K_1^{\frac{1}{3}} V_{V_o}}{\left(\frac{w}{\rho g}\right)^{\frac{1}{3}} \cos^{\frac{1}{3}} \tau}$$

and the theoretical effect of a 24^o vee-step is therefore to decrease the experimental values of B_o given in Fig.6 by 5%.

/Appendix IV .....

TABLE I

Sunderland Mark 5
Data

Hull

Beam (max)	ft.	9.79
Length (F.P. to Rear Step)	ft.	62.12
Length:Beam Ratio		6.35
Forebody Length (F.P. to Main Step Keel)	ft.	32.94
Afterbody Length (Main Step Keel to Aft step)	ft.	29.18
Keel-Chine Deadrise at Main Step		26°
Step Plan Included Angle		132°
Forebody Keel - Hull Datum Angle		3°
Heel - Heel Angle		9° 17'
Forebody Keel - Afterbody Keel Angle		7° 29'
Main Step Fairing Ratio		6:1

Wings

Area (gross)	sq.ft.	1687
Span	ft.	112.8
Incidence to Hull Datum		6° 9'
Section		Gottingen 436 modified

Flaps

Type		Gouge
Area	sq.ft.	286

Tailplane

Area (including elevators)	sq.ft.	205
Elevator area (including tabs)	sq.ft.	84.5
Elevator movement		16° 30' up and down

Engines

4 Pratt Whitney Twin Wasp R.1830-90B giving 1200 B.H.P. at 2,700 r.p.m. and + 9 lb/sq.in. boost for sea level take-off.

Loading

At A.U.Wt. 50,000 lb

C.G. "Normal" is 3.02 ft. forward of main step at keel parallel to hull datum line.

TABLE III

DETAILS OF INDIVIDUAL LANDINGS

Mean A.U.Wt. 50,000 lb

Run No.	Impact No.	V_{v_o} f.p.s.	V_{h_o} f.p.s.	τ Degrees	Angular Velocity deg/sec	dV_n/dt max (g)	t max secs
1	1	6.8	148	2.3	3	0.94	0.38
2	1	6.4	138	5.2	0	1.15	0.40
3	2	5.2	110	9.2	-3	1.21	0.48
4	1	6.5	153	2.0	0	0.94	0.30
5	2	2.9	114	9.8	-4	1.12	0.59
6	1	5.5	140	4.7	+4	1.10	0.38
7	2	3.5	120	9.5	-3	1.02	0.50
8	2	6.8	112	10.3	-5	1.39	0.39
9	1	8.0	142	5.8	+6	1.38	0.33
10	2	3.8	120	9.5	-2	0.80	0.88
11	3	6.3	97	9.9	-4	1.25	0.39
12	1	7.5	129	4.4	+4	1.20	0.34
13	2	4.7	115	9.5	-3	0.97	0.61
14	1	5.0	128	4.2	0	0.70	0.32
15	1	4.7	146	4.7	0	0.69	0.40
16	1	6.0	142	3.5	0	0.81	0.30
17	1	5.8	159	3.2	0	0.80	0.35
18	1	9.0	134	4.6	0	1.40	0.34
19	2	4.6	116	11.8	-8	1.11	0.55
20	2	3.2	109	8.3	-2	0.86	0.78
21	1	5.5	122	11.4	-8	0.95	0.58
22	1	5.6	130	7.0	0	1.2	0.46
23	1	4.1	134	7.0	0	0.67	0.52

/Table IV .....

TABLE IV contd.

Maximum Pressure Results

Run No.	Pick-Up No.	p_{max} p.s.i.	Time to p_{max} - sec	V_v f.p.s.	V_t f.p.s.	τ degs	V_n f.p.s.	$\frac{p_{max}}{(\cot^2\theta + 0.405)}$
17	3	10.0	0.320	2.2	158.4	3.7	12.4	3.0
	8	14.8	0.158	5.4		3.6	15.2	4.7
	9	10.0	0.142	5.5		3.5	15.3	3.2
	15	14.1	0.095	5.6		3.2	14.6	4.4
	16	11.8	0.184	5.0		3.6	14.8	3.2
18	3	17.7	0.206	6.7	133.0	4.8	17.9	5.4
	5	16.5	0.215	6.3		4.8	17.5	4.5
	8	22.5	0.120	8.5		4.4	18.8	7.1
	9	18.5	0.109	8.6		4.4	18.7	5.8
	11	18.2	0.224	6.1		4.8	17.3	4.0
	14	25.0	0.095	8.7		4.4	19.0	7.9
	15	20.0	0.070	8.9		4.4	19.2	6.3
	16	22.1	0.127	8.4		4.4	18.6	6.0
	17	25.1	0.174	7.6		4.7	18.4	5.9
	18	24.5	0.250	5.3		4.8	16.5	4.5
22	9	28.7	0.198	4.5	128.1	7.4	21.3	9.0
	10	29.3	0.276	2.9		7.5	19.9	7.4
	11	33.1	0.368	1.2		8.2	19.8	7.2
	14	27.2	0.150	5.0		7.4	21.7	8.6
	15	25.1	0.135	5.1		7.5	21.9	7.9
	16	30.1	0.173	4.8		7.4	21.5	8.2
	17	37.3	0.236	4.0		7.5	20.9	8.8
	18	29.5	0.329	1.6		7.8	19.1	5.4
23	15	24.5	0.205	3.6	133.3	7.2	20.4	7.7
	16	28.7	0.300	2.7		7.1	19.4	7.8
	17	27.5	0.430	0.9		7.4	18.4	6.5

FIG. 1.

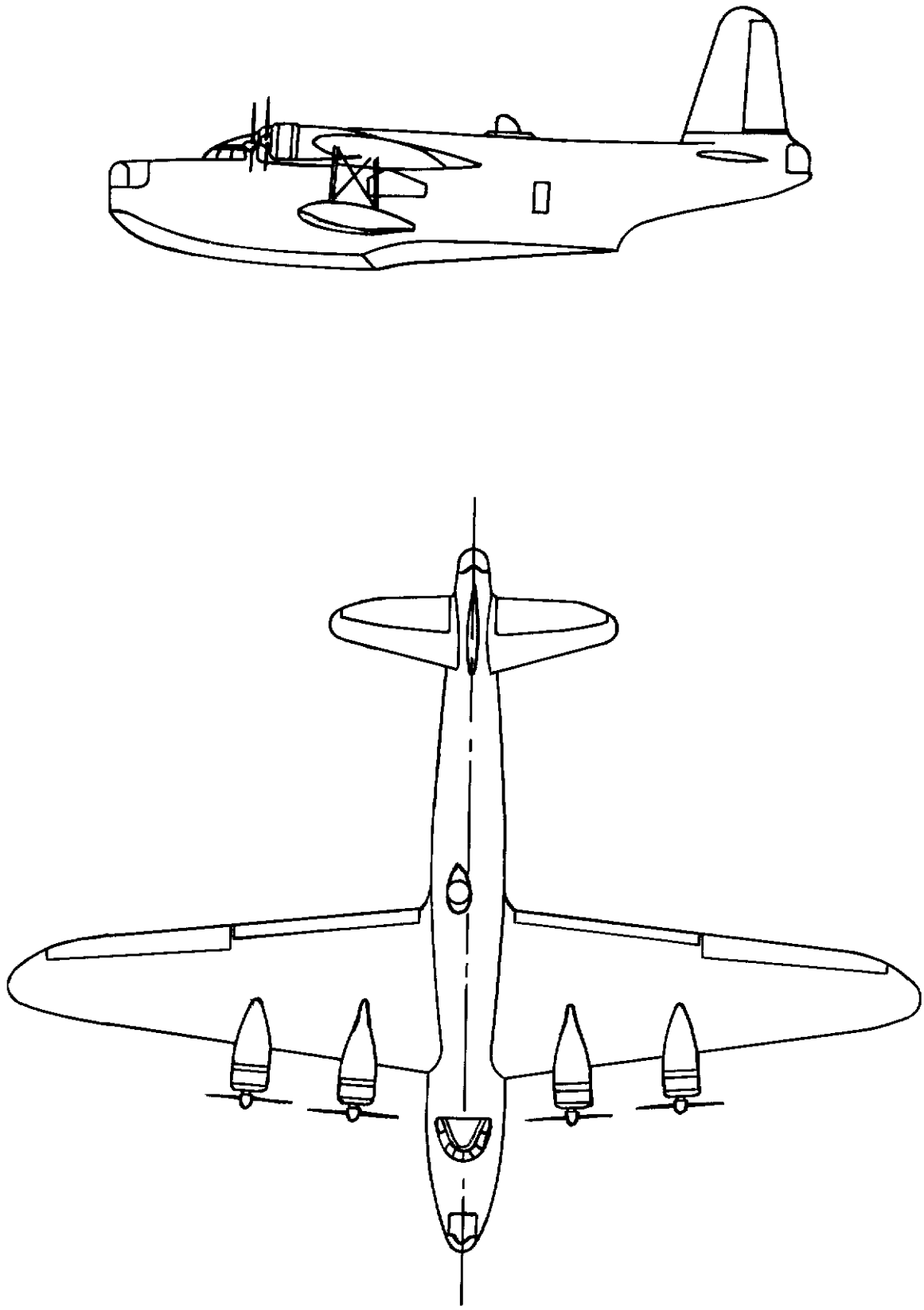

SUNDERLAND MK. 5. FLYING BOAT.

FIG. 3.

PLANING BOTTOM CONTOURS.

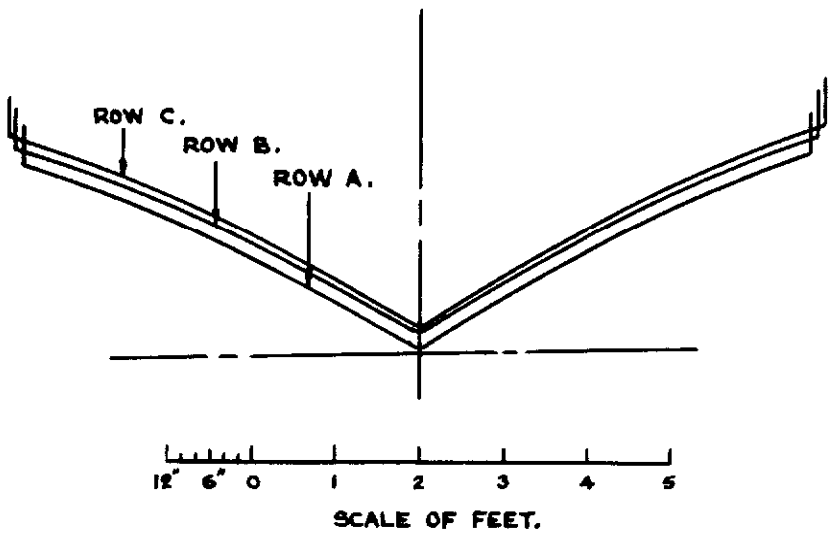

FOR ADDITIONAL DETAILS OF PICK UP POSITIONS SEE TABLE II.

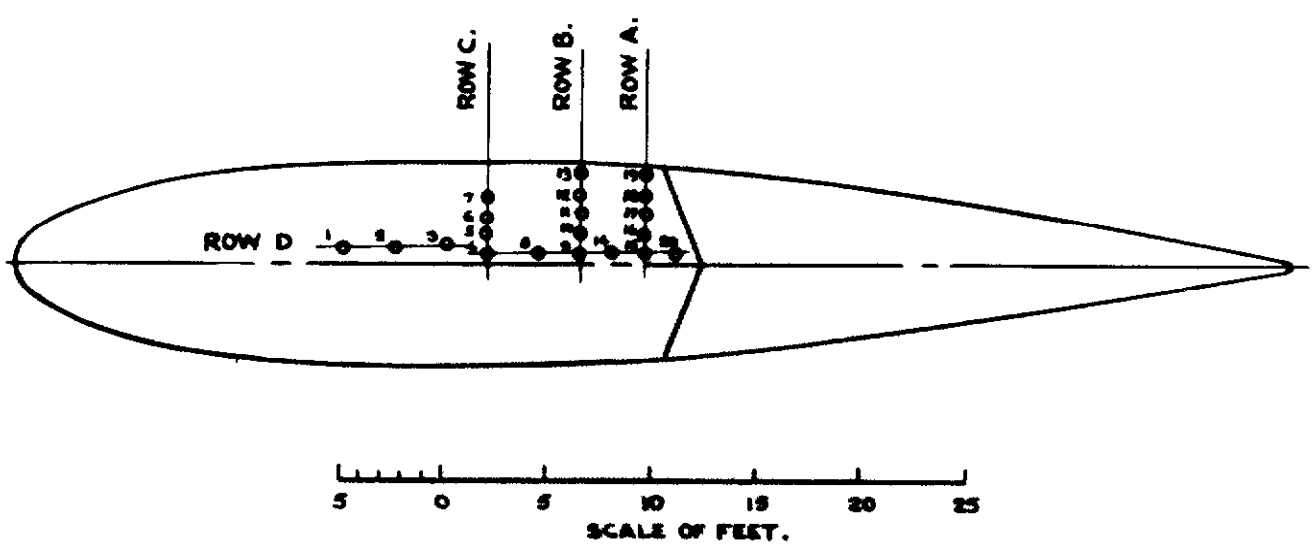

PRESSURE PICK UP POSITIONS

FIG. 4.

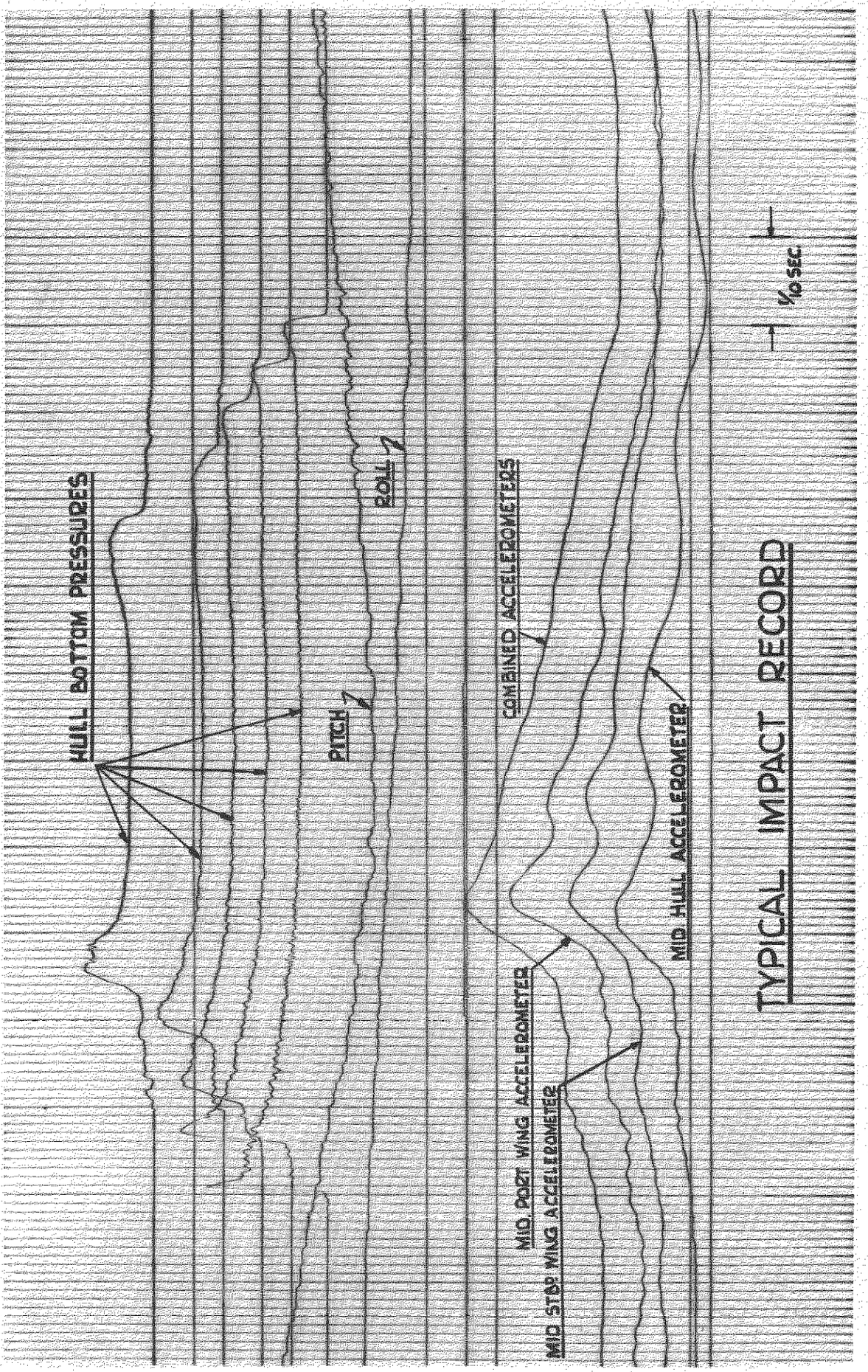

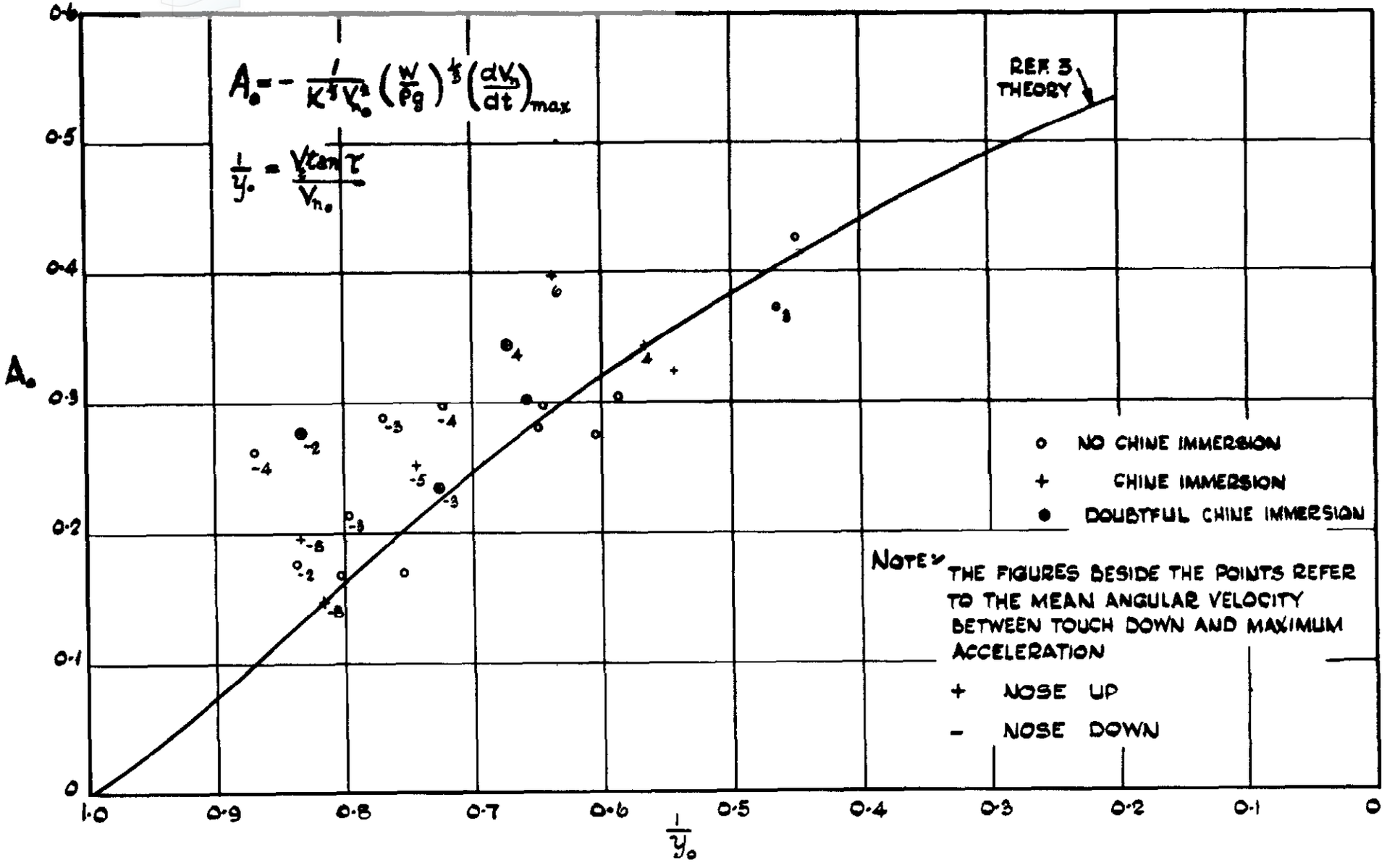

NON DIMENSIONAL PLOT OF MAXIMUM IMPACT ACCELERATIONS

FIG. 5

FIG. 7a

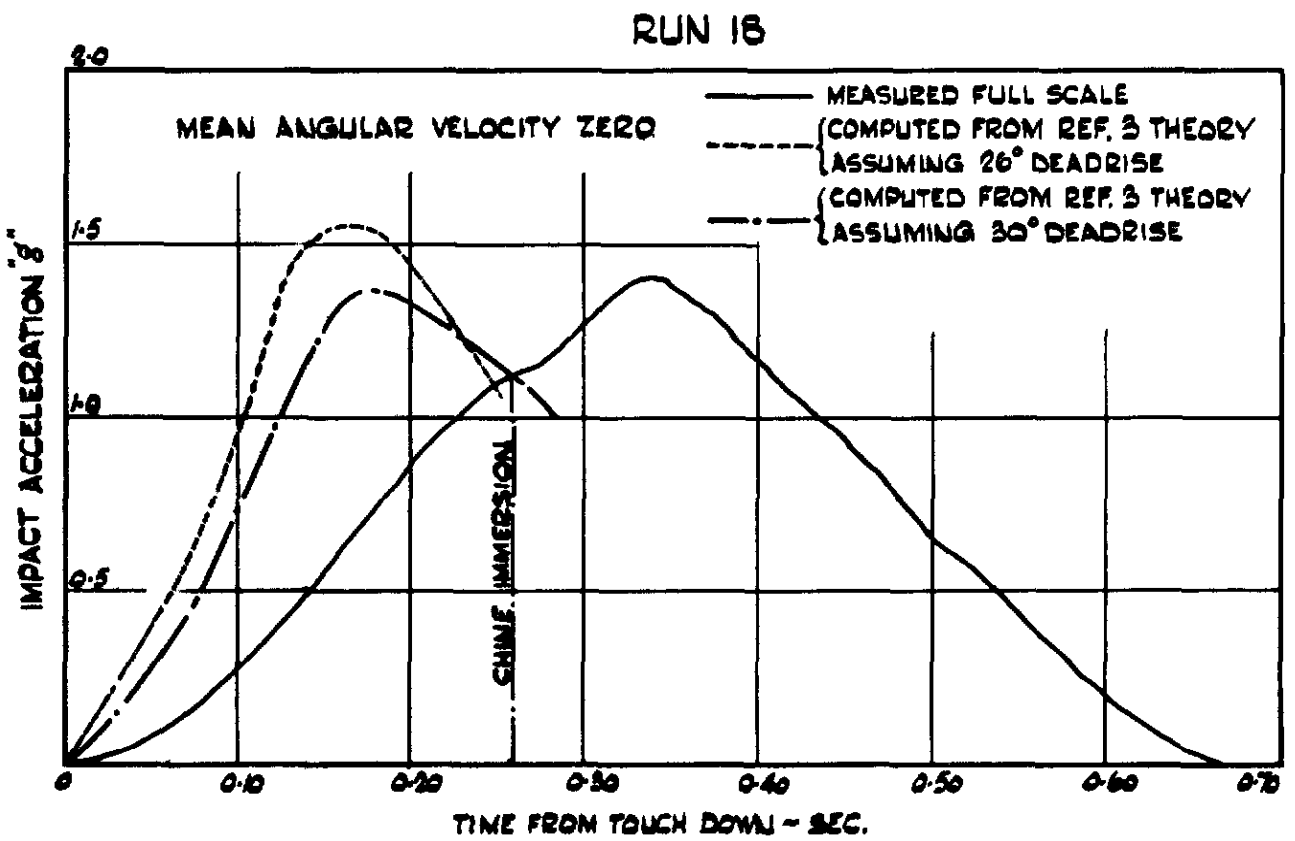

FIG. 7b

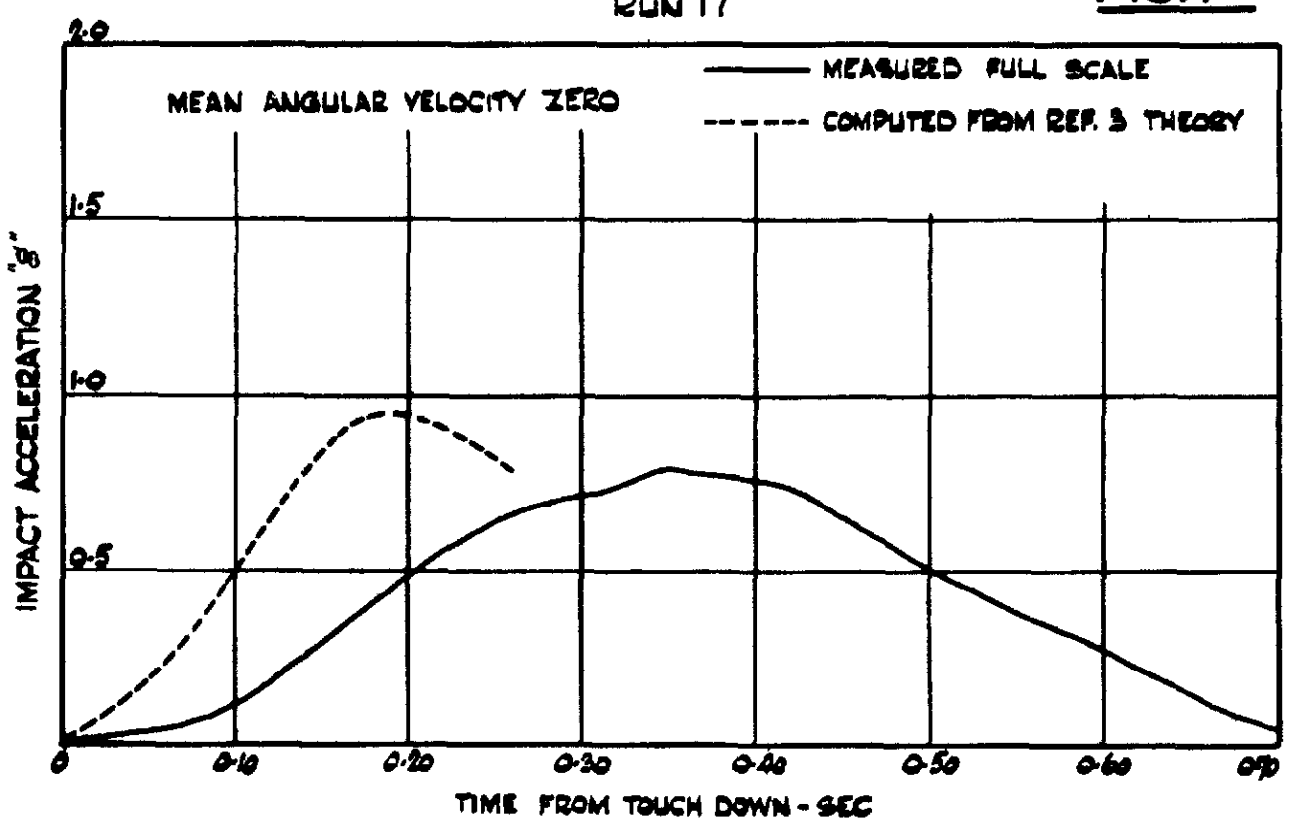

COMPARISON BETWEEN MEASURED AND COMPUTED ACCELERATION-TIME CURVES.

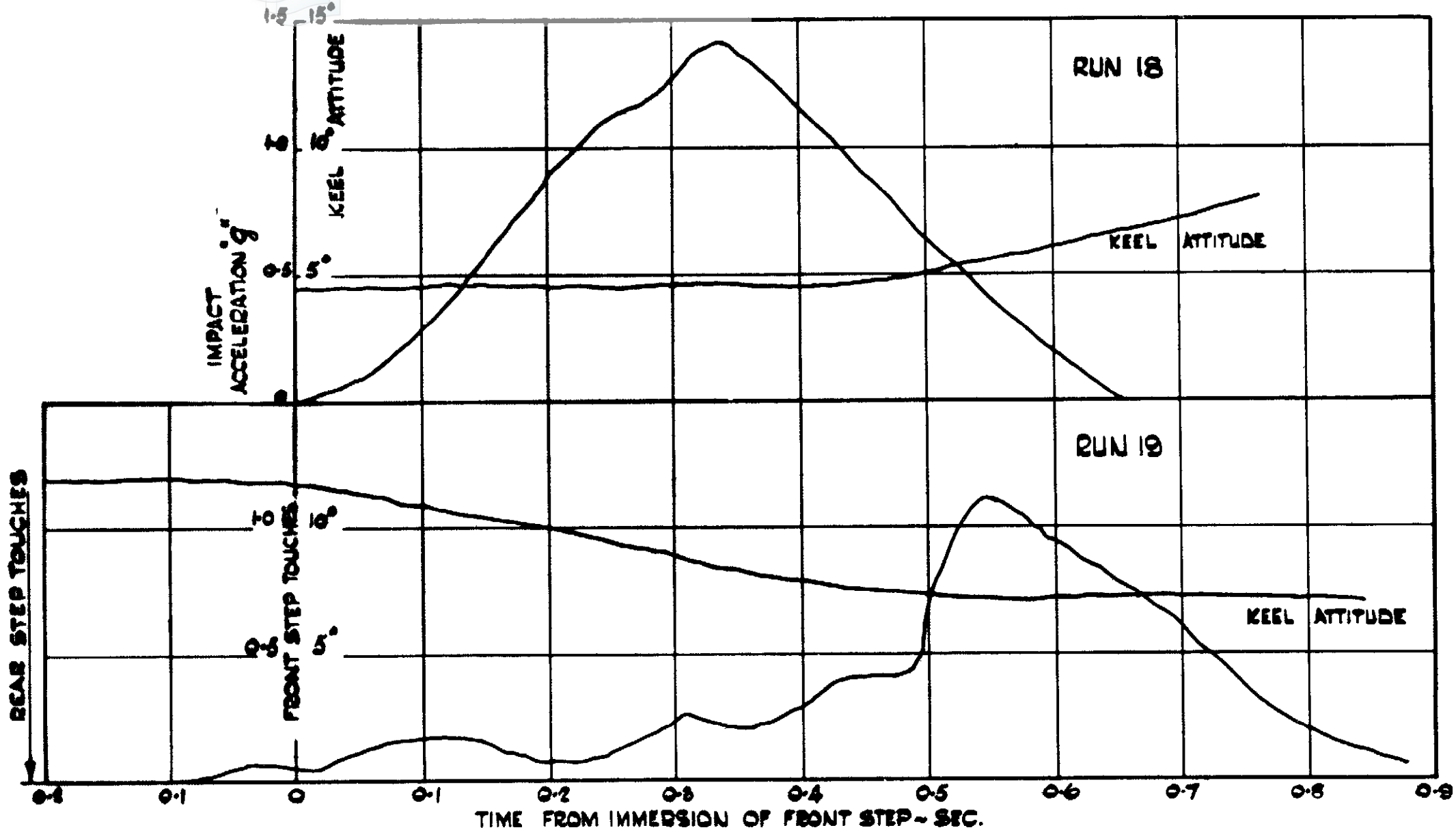

COMPARISON BETWEEN TYPICAL MAIN STEP AND REAR STEP LANDINGS.

FIG. 8

FIG. 9b

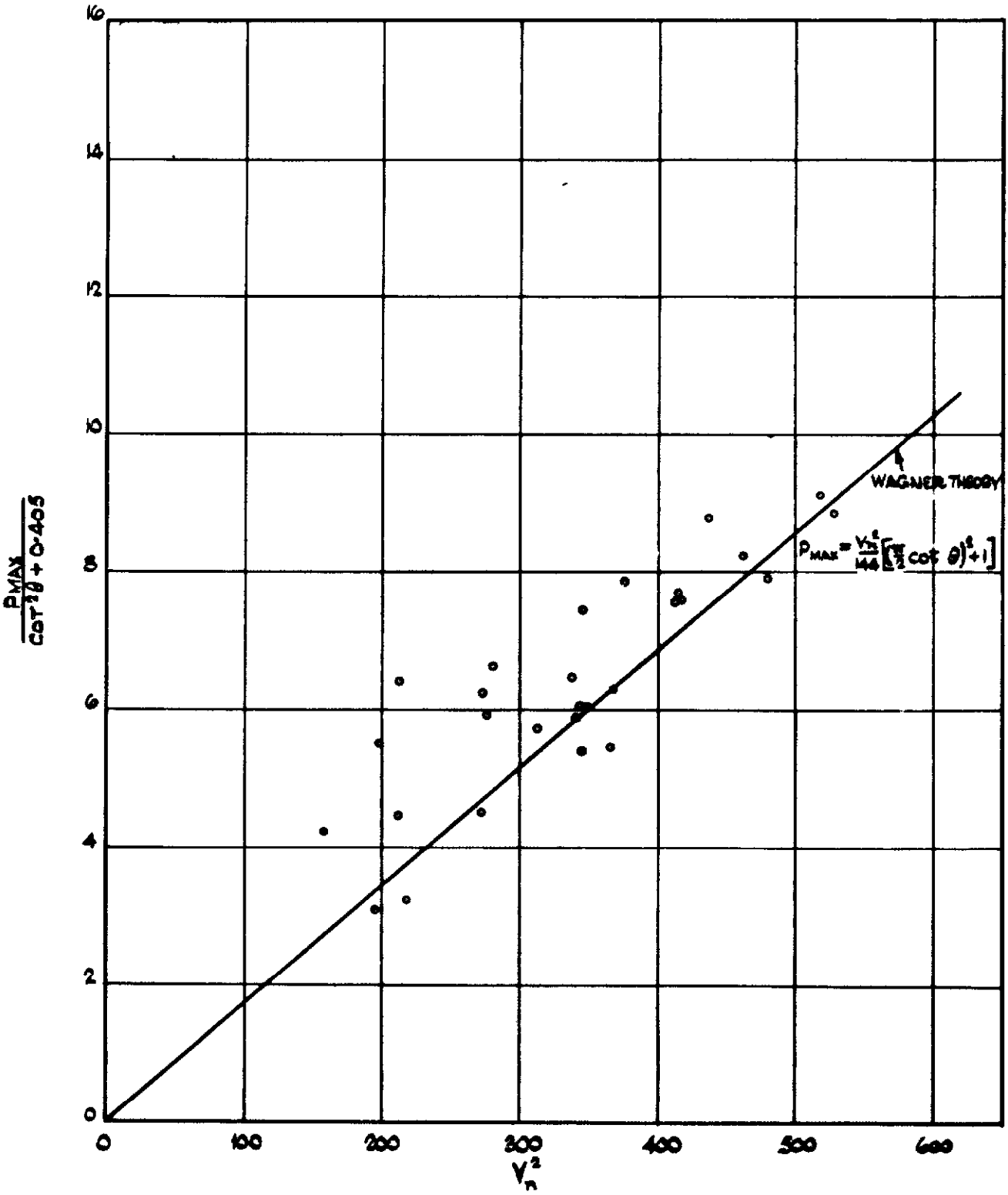

MEASURED MAXIMUM LOCAL PRESSURES.

ROW A.

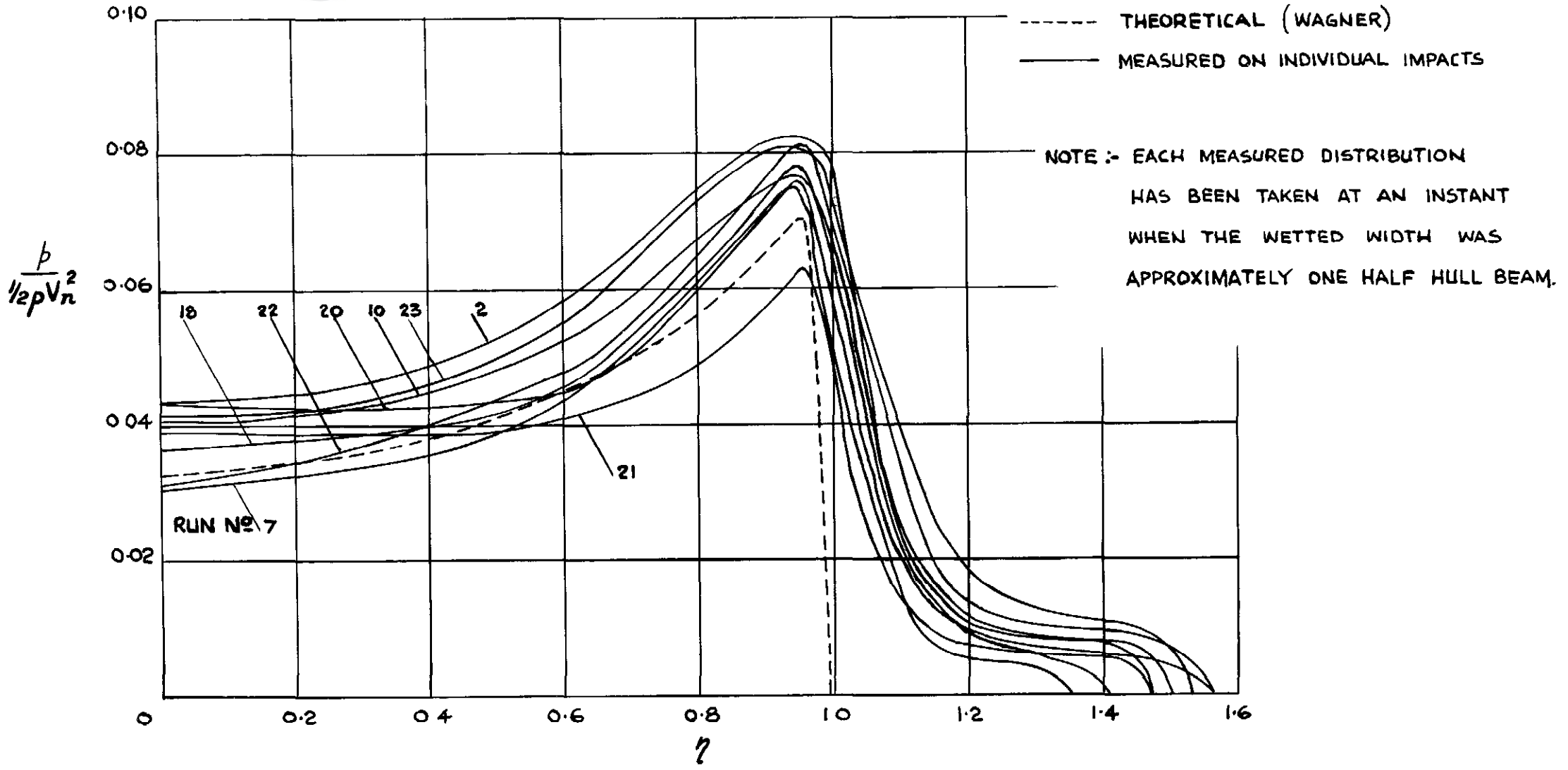

MEASURED TRANSVERSE PRESSURE DISTRIBUTIONS ROW A.

FIG. 10

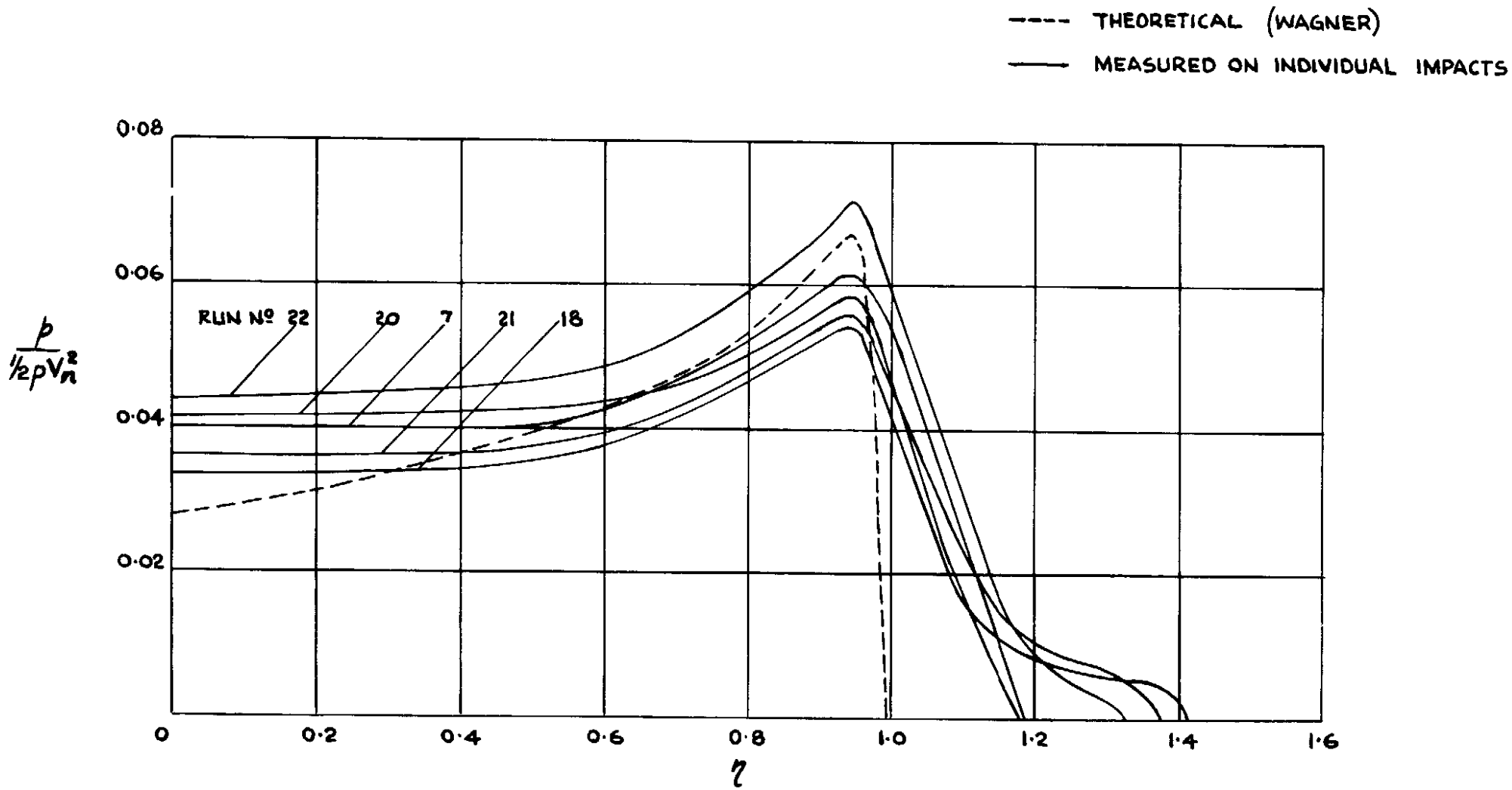

MEASURED TRANSVERSE PRESSURE DISTRIBUTIONS ROW B.

FIG. 12

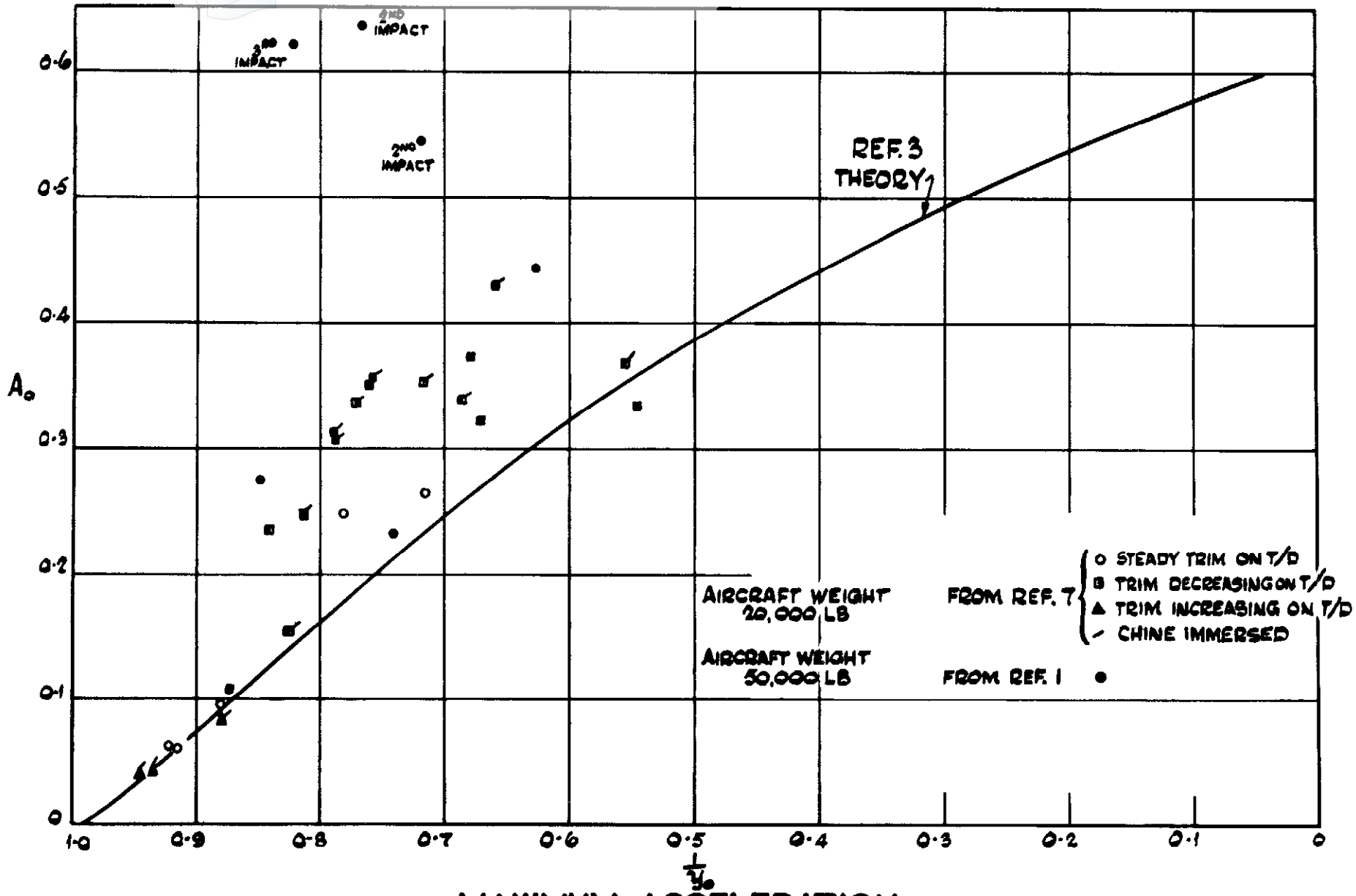

MAXIMUM ACCELERATION
COMPARISON BETWEEN REF 3 THEORY AND EARLIER FULL SCALE TESTS (REF. 7)

FIG. 14

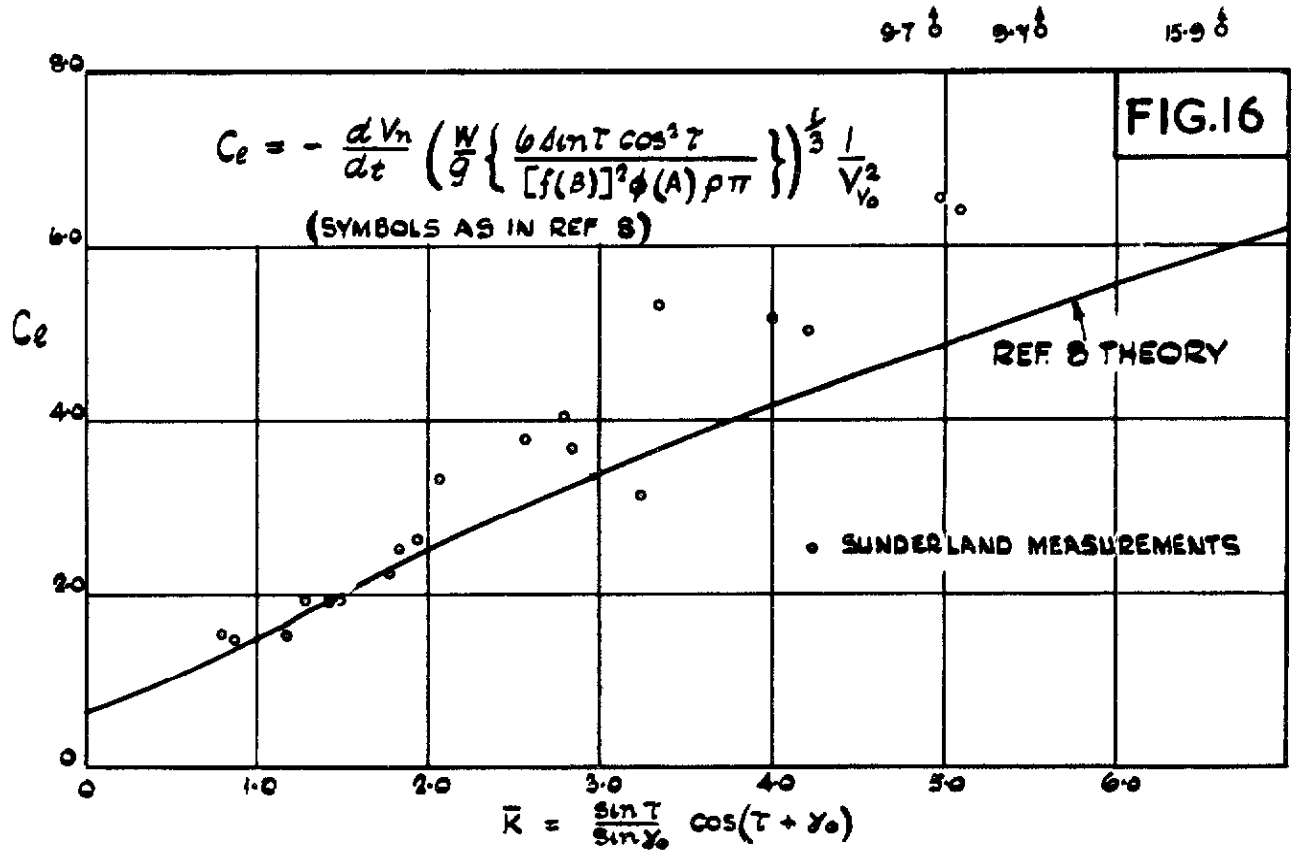

MAXIMUM ACCELERATION
COMPARISON BETWEEN REF. 8 THEORY AND SUNDERLAND FULL SCALE TESTS.

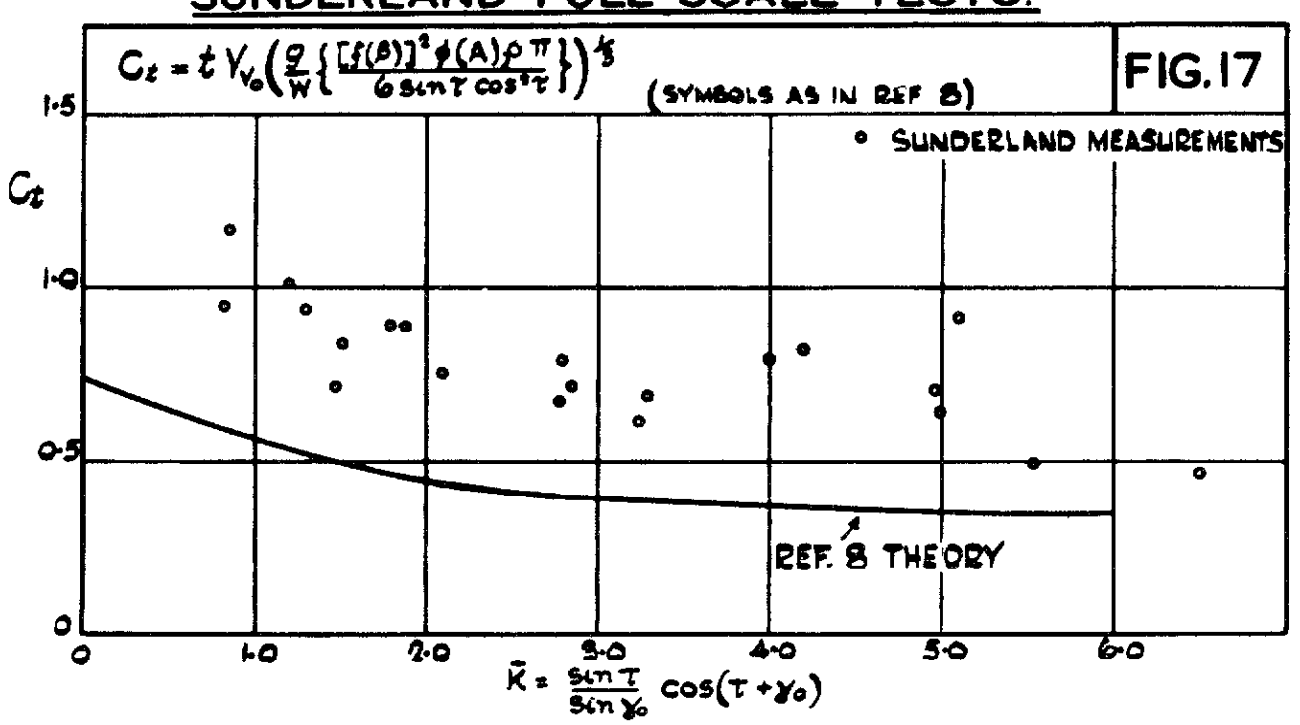

TIME TO MAXIMUM ACCELERATION
COMPARISON BETWEEN REF. 8 THEORY AND SUNDERLAND FULL SCALE TESTS.

FIG.19.

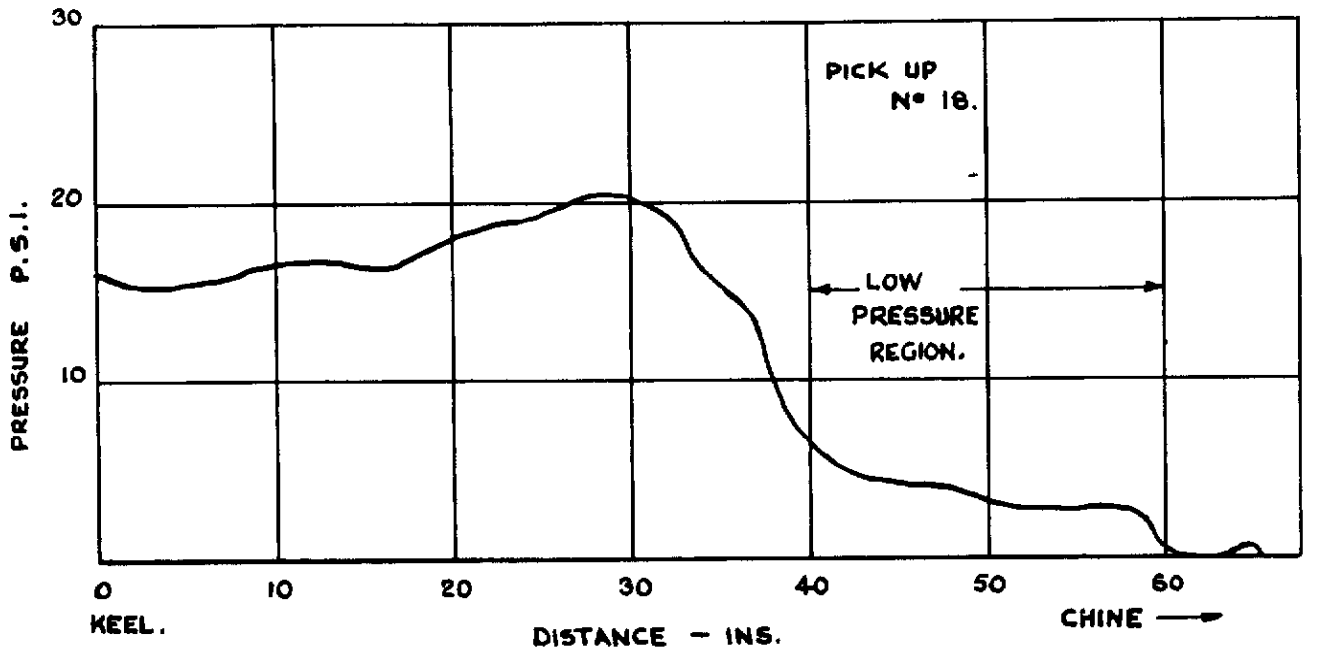

TYPICAL EXAMPLE OF LOW PRESSURE REGION.

FIG.20.

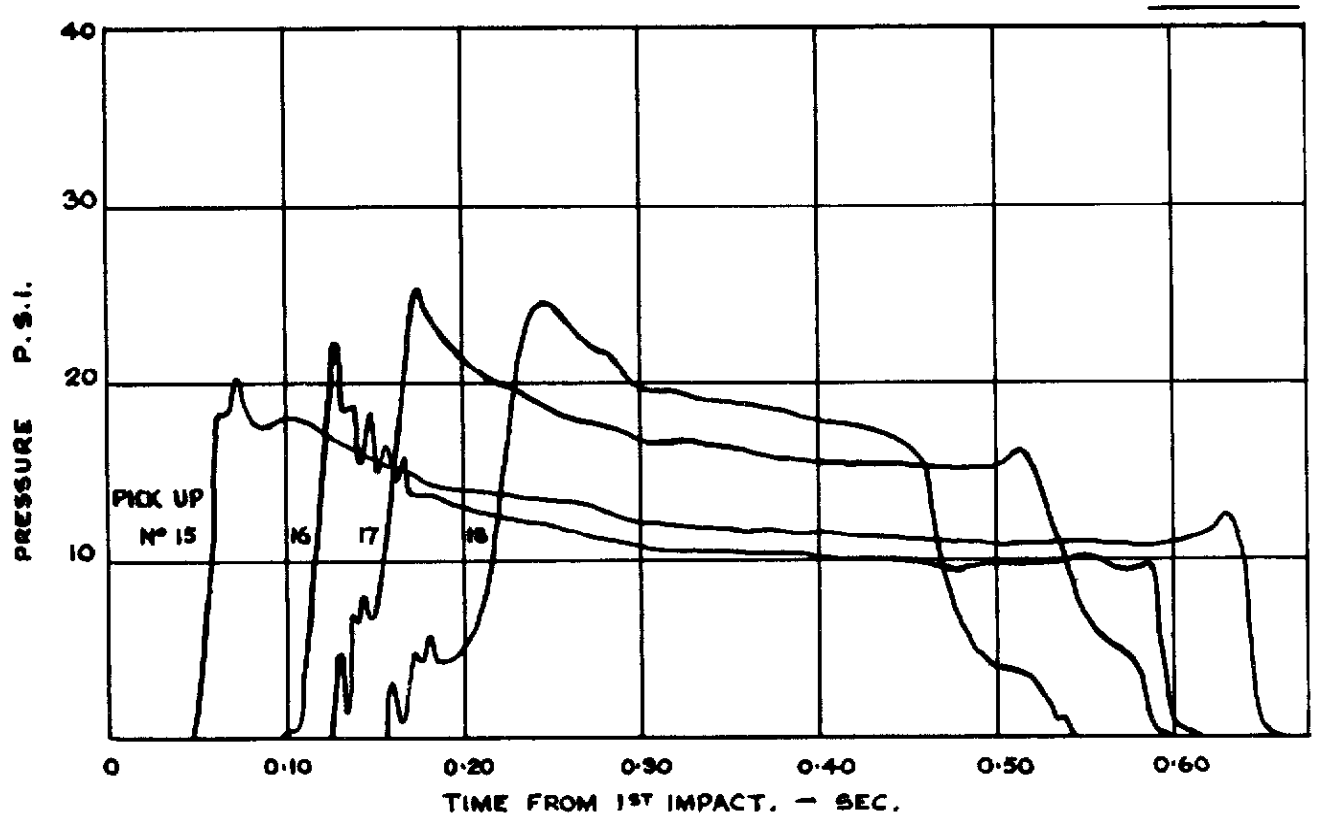

TYPICAL PRESSURE TIME RECORDS FOR ONE IMPACT. (ROW A.)

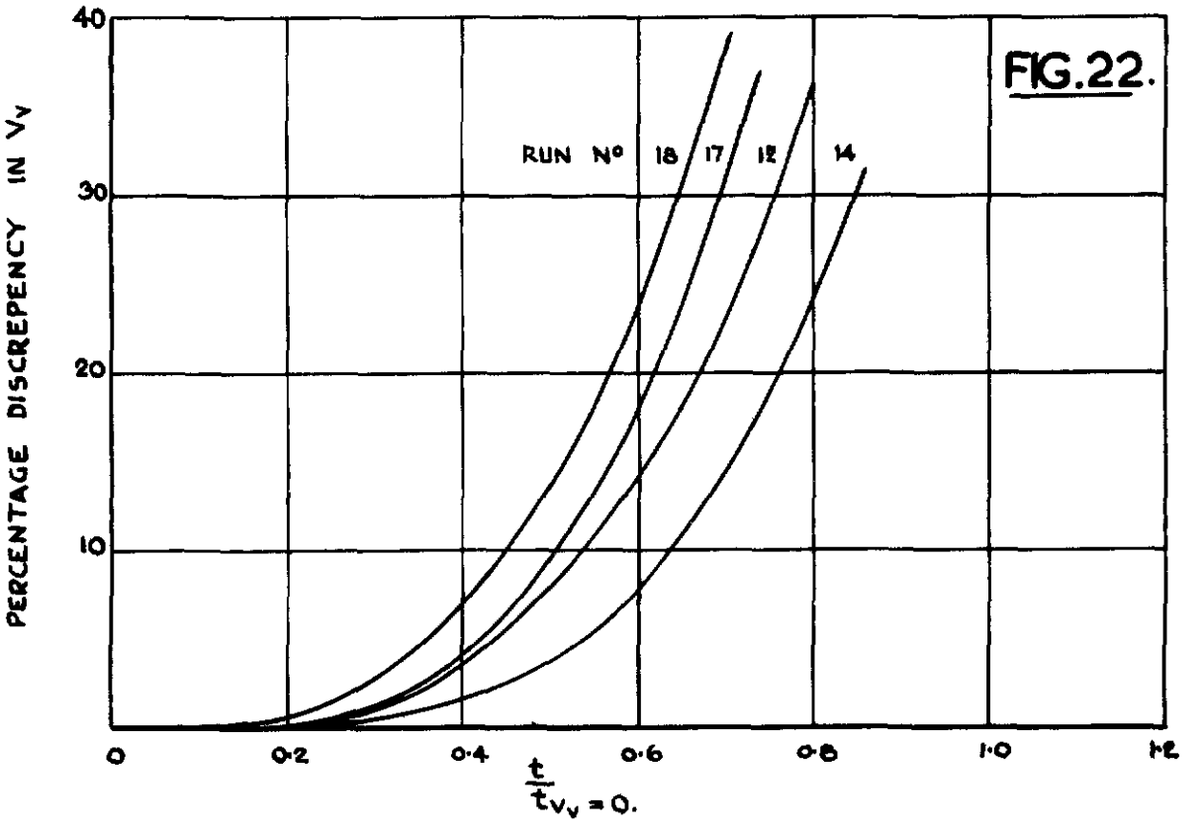

PERCENTAGE DIFFERENCE BETWEEN MEASURED AND THEORETICAL VERTICAL VELOCITIES DURING IMPACT.

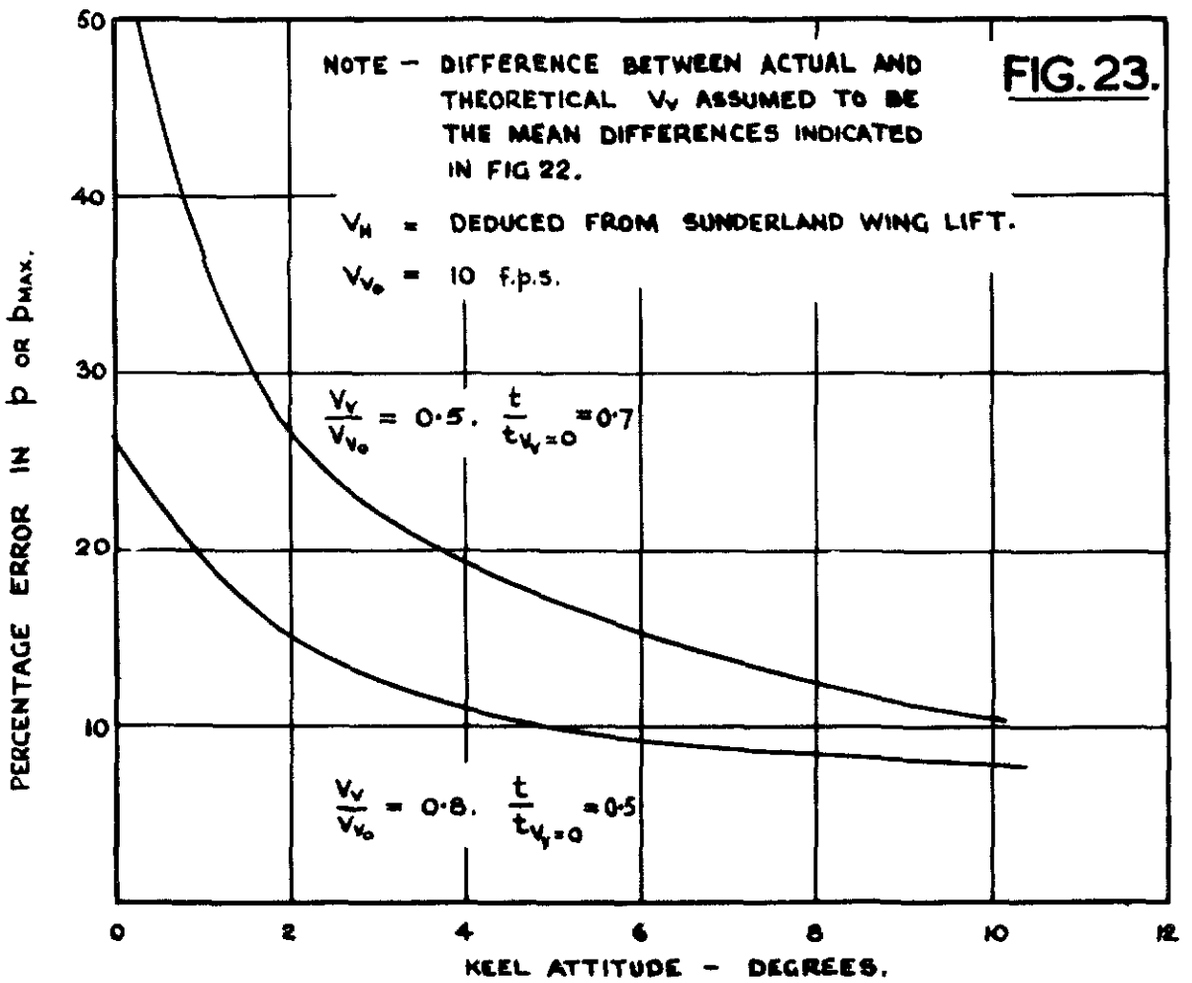

TYPICAL ERRORS IN PRESSURE ESTIMATION.